Relative Effects of Reynolds Number and Freestream Turbulence in Transonic Flow

S. Raghunathan*
The Queen's University of Belfast, Belfast, Northern Ireland, U.K.
and
R. J. W. McAdam†
Short Brothers Ltd., Belfast, Northern Ireland, U.K.

Present herein are the experimental results on the effect of freestream turbulence in the range $0.34\% < Tu_\infty < 3.6\%$ on the pressure distribution over an 18%-thick biconvex airfoil with and without leading-edge trips for a condition corresponding to a significant shock-induced separation. The results are compared with similar measurements on a wall-mounted bump model with a thicker boundary layer at the foot of the shock. The results showed that at low Reynolds numbers the effect of freestream turbulence is primarily through the change in the boundary-layer transition. However, the freestream turbulence had a strong effect on the pressure distribution downstream of the shock interaction at a higher Reynolds number.

Nomenclature

C = chord
C_p = nondimensional pressure coefficient
$C_{p_{TE}}$ = nondimensional pressure coefficient at airfoil trailing edge
$C_{p_{TE_0}}$ = nondimensional pressure coefficient at zero turbulence (extrapolated)
$\Delta C_{p_{TE}}$ = $C_{p_{TE}} - C_{p_{TE_0}}$
$\tilde{e}_f$ = rms voltage at frequency f
f = frequency
h = height of test section
L_x = longitudinal integral length scale (Ref. 8)
M_∞ = freestream Mach number measured 2 chords upstream of airfoil leading edge
M_{PK} = peak Mach number on the airfoil
p_s = static pressure at point of separation
p_1 = static pressure immediately upstream of shock wave
p_0 = stagnation pressure upstream of shock wave
R_θ = Reynolds number based on boundary-layer momentum thickness
Tu_∞ = freestream turbulence intensity $\tilde{u}/U_\infty$
TE = trailing edge of airfoil
U = velocity
$\tilde{u}$ = rms velocity fluctuation
U_∞ = freestream velocity 6 mm upstream of the shock location
X = distance measured from leading edge of the model
X_s = shock position measured from the leading edge of the model
X_{s_0} = shock position measured from the leading edge at zero turbulence (extrapolated)
ΔX_s = $X_s - X_{s_0}$
y = vertical ordinate
Δ_θ = $\theta - \theta_0$
δ = boundary-layer thickness at $u/U_\infty = 0.995$
θ = boundary-layer momentum thickness
θ_0 = boundary-layer momentum thickness at zero turbulence (extrapolated)

Presented as Paper 83-1726 at the AIAA 16th Fluid and Plasma Dynamics Conference, Danvers, Mass., July 12-14, 1983; received July 30, 1983; revision received March 12, 1984.

*Senior Lecturer, Department of Aeronautical Engineering. Member AIAA.
†Research Student, Department of Aeronautical Engineering. Member AIAA.

Introduction

It is well known that model testing in transonic wind tunnels is subjected to Reynolds number and tunnel environmental effects. The Reynolds number effect is discussed in detail by Green,[1] Evans and Taylor,[2] and Pearcey et al.[3] One of the primary variables which describes the tunnel environment is the flow unsteadiness in the tunnel. The flow unsteadiness in transonic tunnels can consist of acoustic pressure fluctuations, turbulence (vorticity), and entropy fluctuations; with the existing experimental techniques it is difficult to separate them. The flow unsteadiness in transonic tunnels can affect boundary-layer transition, the development of turbulent boundary layers, separations, and shock interactions.[4] Although there are several research reports on the effect of flow unsteadiness on boundary-layer transition[4] and attached turbulent boundary layers,[5] there is scant information available as to the effect of flow unsteadiness in general and turbulence in particular on shock interactions.

This paper presents pressure measurements on a 18%-thick biconvex airfoil, with and without transition trips, in transonic flow with significant shock-induced separation at various levels of freestream turbulence. The results are compared with similar experiments on a wall-mounted bump model.

Experiments

The experimental investigations were performend in a 101.6-mm square transonic suckdown intermittent tunnel which had a running time of 15 s. The test section was top and bottom slotted (Fig. 1). The slots were covered with screens to give a porosity of 9.6% based on top and bottom walls. The Mach number in the wind tunnel was measured with a sidewall pressure orifice 2 chords upstream of the model leading edge and was controlled by a downstream choke.

The model was a biconvex airfoil 101.6-mm chord and 18% thick with surface orifices located at 5-mm intervals up to the midchord position and at 2.5-mm intervals between the mid-

chord and trailing edge. The model was located at the tunnel centerline and 622-mm downstream of the turbulence promoting rods. Earlier experiments[5] have shown that the turbulence at this position is free from vortex shedding.

The turbulence-promoting rods were of the vertical monoplane type. The turbulence in the tunnel was varied by varying the diameter and the number of rods, with the blockage at this section being constant for all turbulence levels. A DISA constant-temperature anemometer with a DISA 55P14 hot-wire probe was used for the turbulence measurements. The measurement station for the hot wire was the position corresponding to model location in an empty tunnel. The use of hot wires in transonic flow has been described in Ref. 6.

A pitot probe was used to perform boundary-layer traverses on the model, 6-mm upstream of the shock position, for some of the test cases. Flow separation over the model was detected by the china-clay technique. The flow visualization method of Ref. 7 was used to locate the boundary-layer transition on the model. The boundary-layer trips were made of carborundum grains mixed with adhesive, 4-mm wide and located 3 mm from the leading edge on both sides of the model.

Results and Discussion

The hot-wire spectra of freestream turbulence at the model location for three turbulence levels shown in Fig. 2 show good correlations with the Strouhal number based on the test section height h. A correlation with the Strouhal number based on the diameter of the turbulence promoting rods was found to be poor although such a correlation was very good well upstream of the model location. This indicated that the turbulence measurements at the model location were free from vortex shedding. Experiments with an inclined hot-wire probe revealed that the turbulence was also isotropic.

Approximate estimation of the longitudinal integral scale L_x following Bradshaw[8] based on the boundary-layer thickness δ measured 6-mm upstream of the shock position were within the range $4<L_x/\delta<40$ for the centerline (CL) model. The corresponding range for the wall-mounted (WM) model tests[9] was $1<L_x\delta<6$.

The influence of freestream Mach number on the shock position for the airfoil without the leading-edge trips is shown in Fig. 3. The data shown here are for the freestream turbulence levels $Tu_\infty = 0.34$, 2.18, 3.14, and 3.68%. The plateaus in these curves represent the regions where the rearward movement of the shock is slowed by the onset of shock-induced separation. Onset of separation reduces the shock strength and, therefore, the rearward movement of the shock. This typical behavior is in agreement with that obtained by Pearcey.[10]

For a constant-peak Mach number of 1.44, flow visualization tests showed that, for $Tu_\infty = 0.34\%$, transition occurred at the shock position. The transition moved upstream with the increase in Tu_∞. For values of $Tu_\infty > 3.14\%$ transition occurred near the leading edge of the model. This effect of Tu_∞ on the transition point was also found by Kestin.[11]. This is the reason for the forward movement of the shock when Tu_∞ is increased from 0.34 to 2.18%. For the cases where the boundary layer is fully turbulent from the leading edge ($Tu_\infty > 3.14\%$) an increase in Tu_∞ results in a rearward movement of the shock. It is interesting to note that the shock position is virtually the same for $Tu_\infty = 0.34$ and 3.14% but, as will be seen later, the trailing-edge conditions are different.

The effect of M_∞ on shock position for the case of the airfoil with leading-edge trips is shown in Fig. 4 for various Tu_∞ levels. The boundary layer ahead of the shock was fully turbulent for all of the Tu_∞ results in a rearward movement of the shock. This effect is similar to that observed by the introduction of vortex generators[12] and by moving the transition trip rearward[13] from the leading edge.

The changes in shock position ΔX_s nondimensionalized with respect to the extrapolated value of shock position for

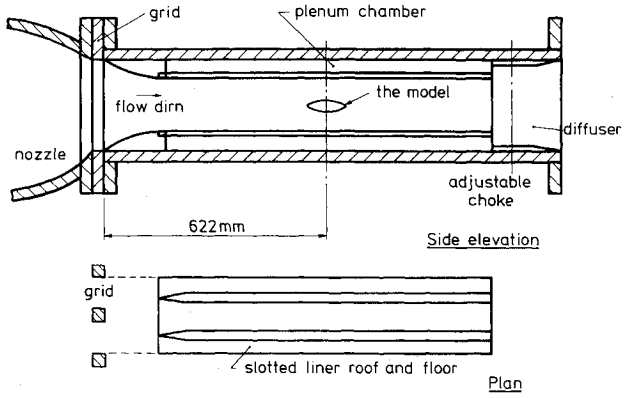

Fig. 1 The slotted test section.

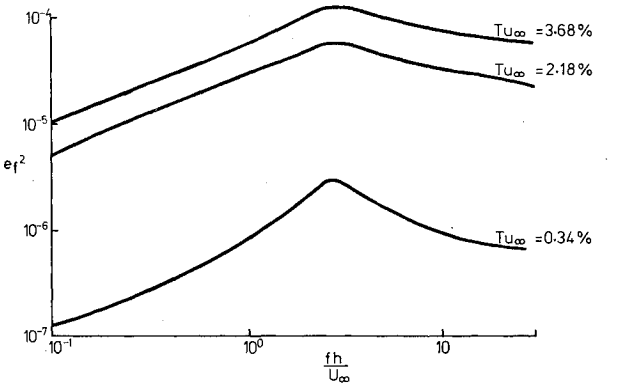

Fig. 2 The spectra of turbulence in the freestream $M_\infty = 0.75$.

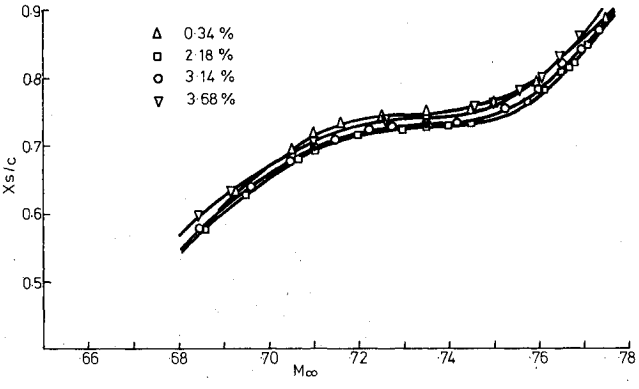

Fig. 3 Variation of shock position with freestream Mach number, airfoil without leading-edge trips.

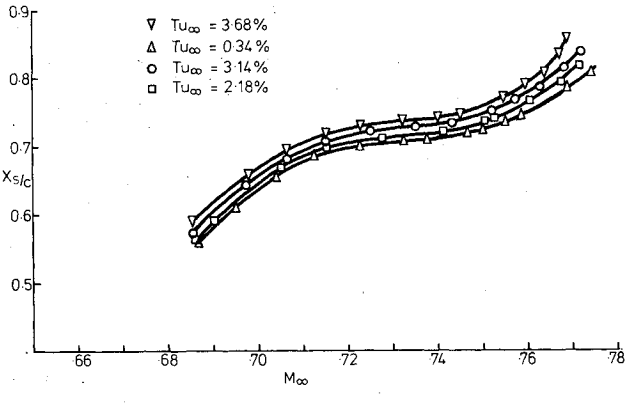

Fig. 4 Variation of shock position with freestream Mach number, airfoil with trips.

$Tu_\infty = 0$, plotted against Tu_∞, for a fixed value of M_∞, for the airfoil with and without trips, are shown in Fig. 5. Also shown here, for comparison, are results from the tests on a WM model[9] where the approaching boundary layer was much thicker. The value of M_{PK} for all of these cases is approximately 1.44, a condition corresponding to significant shock-induced separation. For the airfoil without the leading-edge trips the shock position is very sensitive to Tu_∞. The initial forward movement of the shock with the increase in Tu_∞ is due to the changes in the boundary-layer conditions approaching the shock as mentioned previously. For $Tu_\infty > 3.14\%$ the boundary layer on the surface of the airfoil is fully turbulent from the leading edge and $\Delta X_s/X_{s0}$ is positive. For the airfoil with the leading-edge trips and the WM model, the boundary layer was always turbulent resulting in the rearward shift of the shock position with the increase in Tu_∞.

It also can be observed from Fig. 5 that the WM model results show a larger variation of $\Delta X_s/X_{s0}$ with Tu_∞ when compared with the airfoil with the leading-edge trips mounted in the freestream of the tunnel. This is more noticeable of high values of Tu_∞. It appears that the effect of freestream turbulence is appreciable for the WM model, which has a high Reynolds number and at high turbulence levels.

The pressure distributions over the airfoils without and with the trips for the case of strong shock-induced separation and for a fixed shock position are shown in Figs. 6 and 7 respectively. For clarity, only the results for some values of Tu_∞ are shown. Referring to Fig. 6, the pressure distribution up to the shock position is virtually independent of Tu_∞ or the state of the boundary layer.

However, Tu_∞ has a marked influence on the pressure distribution in the separated region. The boundary layer approaching the shock is laminar for $Tu_\infty = 0.34\%$, resulting in a poor pressure recovery at the trailing edge. Large improvements in pressure recovery occur when the boundary layer becomes fully turbulent from the leading edge ($Tu_\infty = 3.14\%$). The effect of Tu_∞ on the pressure distribution in this region is negligible for $Tu_\infty > 3.14\%$. In fact, Fig. 7 shows that for the case of the fully turbulent boundary layer from the leading edge the effect of Tu_∞ on the pressure distribution downstream of the shock position is very small. Here, the differences in C_p values up to the shock position are due to the differences in M_∞ needed to achieve a constant shock position on the airfoil.

The effect of Tu_∞ on the trailing-edge values of pressure coefficient, nondimensionalized with respect to the values at zero turbulence levels (extrapolated) for the airfoil with and without the leading-edge trips and the WM model can be observed in Fig. 8. The results shown here are for a fixed shock position of $X_s/c = 0.8$ and $M_{PK} \approx 1.44$. The freestream turbulence has only a weak influence on the trailing-edge pressure coefficient at low Reynolds numbers. Obviously Tu_∞

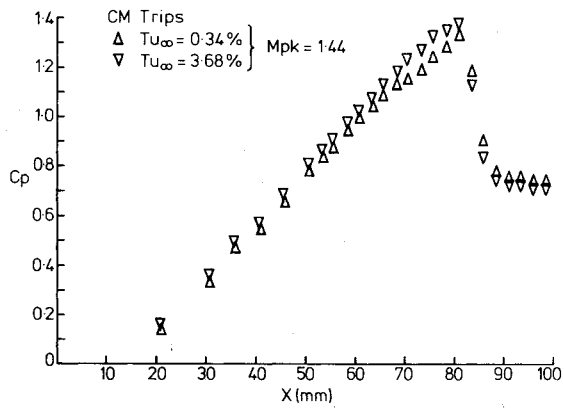

Fig. 7 Pressure distribution over the airfoil for various turbulence levels, with trips.

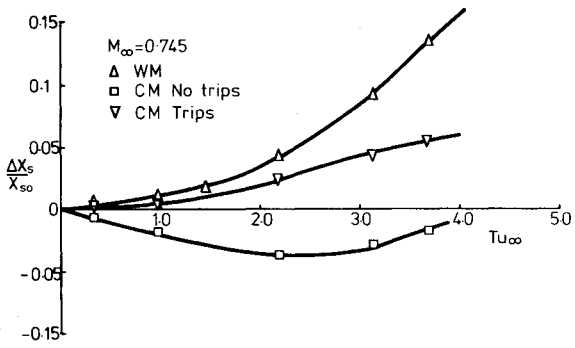

Fig. 5 Effect of freestream turbulence on shock position.

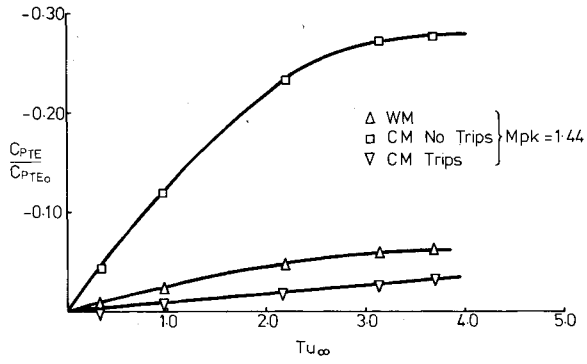

Fig. 8 The effect of freestream turbulence on the trailing-edge pressure coefficient.

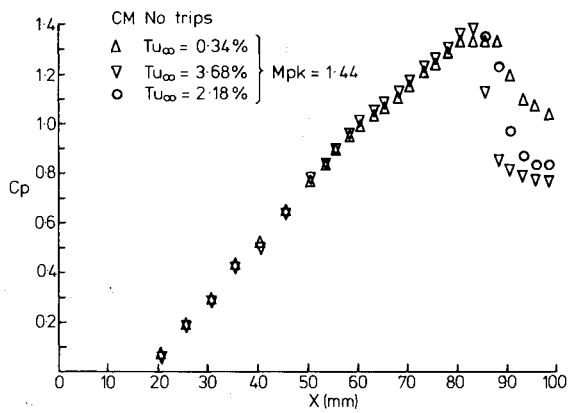

Fig. 6 Pressure distribution over the airfoil for various turbulence levels, without trips.

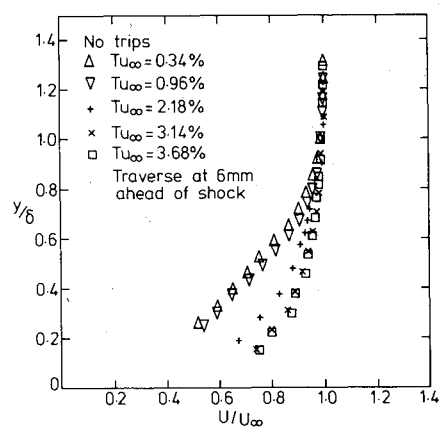

Fig. 9 Velocity profiles upstream of the shock, airfoil without trips.

has a larger affect on C_{pTE} for the airfoil without the leading-edge trips. The trailing-edge values of C_p are very sensitive to the freestream turbulence for the WM model which has a higher Reynolds number.

The velocity profile measurements upstream of the shock wave for the airfoil without and with the leading-edge trips are shown in Figs. 9 and 10, respectively. The changes in the velocity profiles with Tu_∞ for the case of the airfoil without the leading-edge trips is due to the changes in transition location brought about by the turbulence level changes. For the cases where the boundary layer is fully turbulent from the leading edge, $Tu_\infty > 3.14\%$, the velocity profile is rather insensitive to Tu_∞.

The relative influence of Reynolds number and freestream turbulence on the attached boundary layer upstream of the shock interaction can be seen in Fig. 11, where the changes in the boundary-layer momentum thickness nondimensionalized with respect to the corresponding zero turbulence values are plotted against Tu_∞ for the airfoil without and with trips and also for the WM model. It appears from this figure that the boundary layer is sensitive to Tu_∞ only at high Reynolds numbers.

In comparing the CM model results with the WM results it should be noted that the test conditions are not exactly alike. The values of c/h for the CM and WM models are 2 and 1 respectively. The effective freestream Mach number for the CM model is higher than that for the WM model due to blockage effects. This could account for the absolute values shock position for a given value of Tu_∞ but is not likely to affect the relative changes in $\Delta X_s/X_{s0}$ with Tu_∞. The WM model is subjected to the upstream history of the turbulent boundary layer growing on the tunnel wall which is influenced by the changes in Tu_∞. The effect of increasing Tu_∞ on such a boundary layer is to increase the boundary-layer thickness upstream of the shock wave. This, in turn, will have the effect of moving the shock forward but the experiments have shown that the effect of increasing Tu_∞ is to move the shock rearward. The WM model has a trailing condition significantly different from the CM model and the effect of Tu_∞ on the shock/boundary-layer interaction could be considerably larger with the presence of a surface at the trailing edge. The WM model also suffers from a large three-dimensional effect as the boundary-layer thickness on the model is of the same order as that on the tunnel sidewall and the effect of freestream turbulence on the interaction could also be modified by the three-dimensional effects. One plausible explanation is that, whereas the length scales of turbulence are of the same order as the boundary-layer thickness for the WM model, they are an order of magnitude larger for the CM model and, therefore, should have a weaker influence on the CM model as suggested in Fig. 11.

Studies[10] on the effect of Tu_∞ on heat transfer from circular cylinders and flat plates have shown tht freestream turbulence primarily affected the point of transition at low Reynolds numbers as also observed by Consigny and Richards.[14] However, McDonald and Kreskovsky[15] have shown by comparison of theory and experimental data that Tu_∞ has a small effect at low R_θ values and a larger effect at high R_θ values. They quote a watershed value of $R_\theta \sim 5000$. It is interesting to note that this value lies midway between the present results ($R_\theta \sim 2000$) and the WM model results[13] ($R_\theta \sim 8000$). Thus, it is believed this Reynolds number effect on Tu_∞ is evidenced in Fig. 11. The Reynolds number effect is also evident in the experiments of Charnay et al.,[16] Kline et al.,[17] and Commings et al.[18] Earlier experiments by the authors[4] on a flat-plate boundary layer was at a value of $R_\theta = 10{,}000$ and showed a strong effect of freestream turbulence.

Figure 12 shows the pressure rise to separation in the form of a plot of p_s/p_{0l} vs p_l/p_{0l}. The experimental data shown here are from the present tests, from the previous tests on a WM model,[9] and those taken from Ref. 20.

The theoretical predictions for a normal shock-wave and shock-induced separation from Holder and Gadd[21] for a flat-plate turbulent boundary-layer interaction are also shown for comparison.

It is clear from the plot that the pressure rise to separation is enhanced by Tu_∞ both for the thin and thick boundary layers, but the increase in pressure rise is appreciable only for thick boundary layers. It is also observed that for a given Tu_∞ the thicker boundary-layer results in a lower pressure recovery. This boundary-layer thickness effect was also observed by Little.[22] The discrepancy between the theory for a normal shock and the experimental data on the airfoils is lower than that expected theoretically due to the relative differences in the

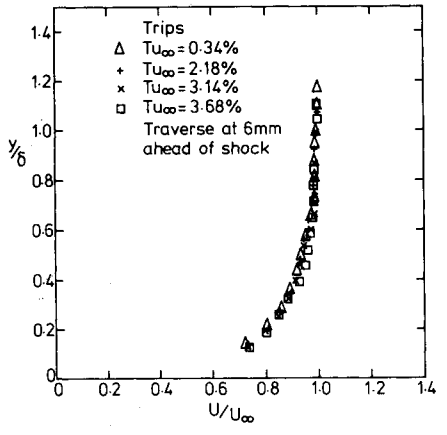

Fig. 10 Velocity profile upstream of the shock, airfoil with trips.

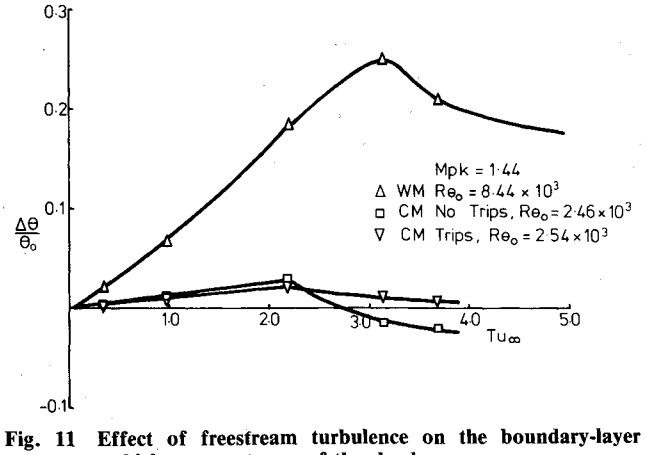

Fig. 11 Effect of freestream turbulence on the boundary-layer momentum thickness, upstream of the shock.

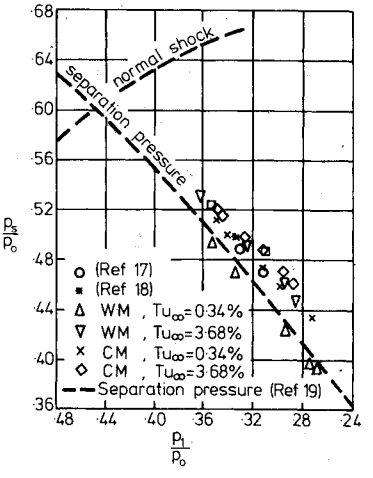

Fig. 12 Pressure rise to separation.

boundary-layer condition and the relative abrupt expansion following the shock.

Conclusions

Experimental results on the effect of freestream turbulence in the range $0.34\% < Tu_\infty < 3.68\%$ on the pressure distribution over an 18% thick biconvex airfoil and a wall-mounted airfoil showed that at low Reynolds number of $R_\theta = 2500$ the effect of freestream turbulence is primarily through the change in the boundary-layer transition. The freestream turbulence appears to have a strong effect on the pressure distribution downstream of the shock interaction at a higher Reynolds number of $R_\theta = 8000$ and more experiments are needed to confirm this.

References

[1]Green, J. E., "Some Aspects of Viscous-Inviscid Interactions at Transonic Speeds and Their Dependence on Reynolds Number," AGARD-CP-81, Paper 2, 1971.

[2]Evans, J. Y. G., and Taylor, C. R., "Some Factors Relevant to the Simulation of Full Scale Flows in Model Tests and to the Specification of New High Reynolds Number Transonic Tunnels," AGARD-CP-53, Paper 31, 1971.

[3]Pearcey, H. H., Osborne, J. J., and Haines, A. B., "The Interaction Between Local Effects at the Shock and Rear Separation—A Source of Significant Scale Effects in Wind Tunnel Tests on Airfoils and Wings," AGARD-CP-35, Paper 11, 1968.

[4]Timme, A., "Effects of Turbulence and Noise on Wind Tunnel Measurements at Transonic Speeds," AGARD-R-602, Paper 5, 1973.

[5]Raghunathan, S., and McAdam, R. J. W., "Free Stream Turbulence and Attached Subsonic Turbulent Boundary Layers," AIAA Paper 82-0029, Jan. 1982.

[6]Rose, W. C., and McDaid, E. P., "Turbulence Measurements in Transonic Flow," *AIAA Journal,* Vol. 15, Sept. 1977, pp. 1368-1370.

[7]Richards, E. J., and Burstall, F. H., "The China Clay Method of Indicating Transition," ARC TR T&M 2126, 1945.

[8]Bradshaw, P., "Effect of Free Stream Turbulence on Turbulent Shear Layers," Imperial College, London, Aero Report 74-10, Oct. 1974.

[9]Raghunathan, S., and McAdam, R. J. W., "Free Stream Turbulence and Transonic Flow over a Bump Model," *AIAA Journal,* Vol. 21, April 1983, pp. 503-508.

[10]Pearcey, H. H., "Some Aspects of Shock Induced Separation of Turbulent Boundary Layers in Transonic Flow Past Airfoils," ARC R&M 3108, 1959.

[11]Kestin, J., "The Effect of Free Stream Turbulence on Heat Transfer Rates," *Advances in Heat Transfer,* Vol. 3, 1966, pp. 1-32.

[12]Donaldson, C du P., "Investigation of a Simple Device for Preventing Separation Due to Shock and Boundary Layer Interaction," NACA RM L50 B02, Nov. 1950.

[13]Loving, D. L., "Wind Tunnel-Flight Correlation of Shock Induced Separated Flow," NASA TN D-3580, 1966.

[14]Consigny, H., and Richards, B. E., "Short Duration Measurements of Heat Transfer Rate to a Gas Turbine Rotor Blade," ASME Paper 81-GT-146, 1981.

[15]McDonald, H., and Kreskovsky, J. P., "Effect of Free Stream Turbulence on the Turbulent Boundary Layer," *International Journal of Heat and Mass Transfer,* Vol. 17, 1974, pp. 705-716.

[16]Charnay, G., Compte-Bellot, and Mathieu, J., "Development of a Turbulent Boundary Layer on a Flat Plate in an External Turbulent Flow," AGARD-CP-93, Paper 27, 1971.

[17]Kline, S. J., Lisin, A. V., and Waitman, B. A., "Preliminary Investigation of Effect of Free Stream Turbulence on Turbulent Boundary Layer Growth," NASA TN-368, 1960.

[18]Commings, E. W., Clapp, J. T., and Taylor, J. F., "Air Turbulence and Transfer Processes," *Journal of Industrial Engineering Chemistry,* Vol. 40, June 1948, pp. 1076-1082.

[19]Delery, J., "Some Features of Transonic Shock Wave Turbulent Boundary Layer Interaction," von Kármán Institute, Brussels, LS 1980-8.

[20]Levy, L. L., "Experimental and Computational Steady and Unsteady Transonic Flows about a Thick Airfoil," *AIAA Journal,* Vol. 16, June 1978.

[21]Holder, D. W., and Gadd, G. E., "The Interaction Between Shock Waves and Boundary Layers and its Relation to Base Pressure in Supersonic Flow," *Proceedings of the Symposium on Boundary Layer Effects in Aerodynamics,* Paper 8, National Physical Laboratory, England, March 1955.

[22]Little Jr., B. H. "Effects of Initial Turbulent Boundary Layer on Shock Induced Separation in Transonic Flow," von Kármán Institute, Brussels, TN 39, Oct. 1969.